1 Corrosion Protection Function and Breakdown Mechanism of Passive Films on Stainless Steels

Katsuhisa Sugimoto

1.1 Introduction

Stainless steels are Fe-Cr-based alloys containing more than 12% Cr (%: mass percent). The corrosion resistance of the steels depends on passive films mainly composed of Cr-oxyhydroxide. In order to understand the properties of passive films, many studies concerning the structure and composition of the films have been extensively performed [1]. Since these steels are usually used in aqueous environments, much effort has been directed towards in-situ analysis of the passive films formed in these environments [2]. As a result, the relationship between the corrosion resistance and the properties of passive films has been revealed, at least in fundamental corrosive environments [1–3].

Passive films on stainless steels are, however, heterogeneous and they have many compositional and structural defects. Therefore, it is difficult to obtain a definitive answer to corrosion problems when the corrosion results from microscopic defects in the films because analytical techniques usually measure only average composition over a relatively wide analytical area. In order to cope with such situations, an experimental technique that analyzes electrochemical properties of artificially synthesized films with various compositions in a composition range close to real passive films was begun [4,5]. Artificially synthesized passive films are called artificial passivation films. Studies using artificial passivation films have been very effective in revealing the relationship between film composition and electrochemical property [5].

Among the many types of corrosion on stainless steels, pitting is very dangerous because it arises easily in chloride-containing aqueous environments and penetrates the wall of stainless steel containers or pipes. Pitting is believed to arise at microscopic defects in a passive film. The substance of the defects and the breakdown mechanism of passive films at the defects are, however, still unclear. In this chapter, concerning pitting on Fe-Cr alloys in acidic chloride solutions, conditions for the exhibition of corrosion protection function and, in contrast, for the occurrence of breakdown will be explained for passive films on the alloys based on the results of recent studies using artificial passivation films.

1.2 Origin of Pit Initiation

In pit initiation on commercial stainless steels in neutral chloride solutions, it is well known that non-metallic inclusions in the steels, such as MnS, play an important role [6–10]. However, this chapter covers pitting on high purity stainless steels and does not consider the effect of non-metallic inclusions. Pitting occurs on stainless steel thin films formed by sputtering deposition [11, 12]. This suggests that the breakdown of passivity is one of origins of pit initiation. On the other hand, whether the passive film can exist stably in acidic chloride solutions determines whether a pit, i.e. a corrosion cavity caused by pitting, can be repassivated. Therefore, this chapter focuses on the suppression mechanism of passive film breakdown by Cr in Fe-Cr alloys.

1.3 Suppression Mechanism of Passive Film Breakdown by Alloyed Cr

The threshold Cr content above which high purity Fe-Cr alloys become immune against pitting in acidic chloride solutions can be determined by the anodic polarization curve of the alloys with a series of Cr content in 1 M HCl. Figure 1.1 shows one of examples of such polarization curves [13]. Similar measurements have been reported in the literature [14, 15]. The results reported indicate that steels become immune against pitting in 1 M HCl when their Cr content exceeds 30% [13–15].

Concerning the role of Cr in the inhibition of passive film breakdown on Fe-Cr alloys in acid chloride and other electrolyte solutions, many theories

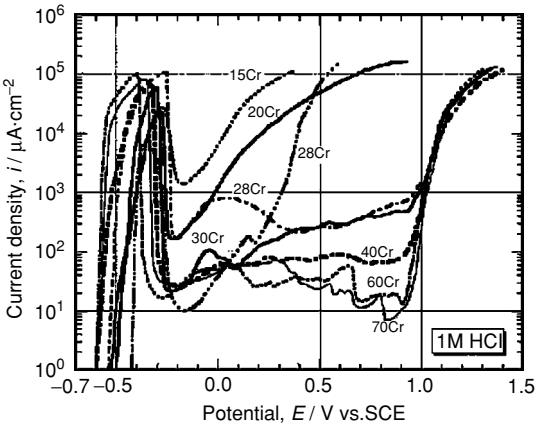

Fig. 1.1. Aodic polarization curves of Fe-Cr alloys in 1 M HCl [13]

have been proposed:

(1) Micro-pore repassivation model [16]: Cr interferes with the development of micro-pores in passive films due to rapid repassivation by the formation of passive Cr-oxyhydroxide film.
(2) Bipolar model [17]: CrO_4^{2-} enriched at the interface between an Fe-rich outer layer and a Cr-rich inner layer bipolarizes the passive film and impedes the ingress of Cl^- ions.
(3) Percolation model [11, 12, 18–20]: Cr forms a passive oxide that is a completely connected structure via first and second nearest neighbor Cr atoms in the original bcc lattice.
(4) Repassivation enhancement model [21, 22]: Cr enhances repassivation through the formation of Fe-Cr oxychloride salt films at the interface of the alloy under which passive films are formed.
(5) Cr-oxide enriched barrier layer model [23]: Cr-oxide increases in the oxide layer near the film/alloy interface, forming a more protective barrier layer.
(6) Fe_2O_3-component reduction suppression model [24, 25]: Cr suppresses the reductive dissolution of the Fe_2O_3-component in passive films which leads to passive film breakdown.

The basic ideas of the suppression of the chloride pitting by the Cr addition in models (1), (3), (4) and (5) are based on the formation of a Cr-like passive film which is immune against chloride pitting. That is, these models assume that, when an alloy is covered by such a film, the alloy becomes immune against pitting. However, the reason why the Cr-like passive film is immune against pitting should be explained from a functional viewpoint of film. Models (2) and (6) are explanations based on the function of film. However, model (2) is hard to apply to pitting in acid chloride solutions that originates at lower potentials than the transpassive dissolution potential of Cr. The last model (6) was first proposed by the authors to explain the suppression of chloride pitting by Mo on Fe-Cr-Mo alloys based on simulation experiments using artificial passivation films [24]. The model was later proved to be applicable to the suppression of pitting by Cr on Fe-Cr alloys [25]. The suppression of pitting will be explained using this model in the following sections.

1.4 Composition of Passive Films Formed in Acid Chloride Solutions

It is important at first to clarify what kind of passive film is immune against pitting in acid chloride solutions. As stated above, Fe-Cr alloys containing more than 30% Cr suffer from no pitting in 1 M HCl. Results of X-ray photoelectron spectroscopic (XPS) analysis of passive films formed on Fe-19Cr [16] and Fe-30Cr [14] alloys at various potentials in 1 M HCl have been reported. Figure 1.2 shows cationic fraction as a function of potential for the passive

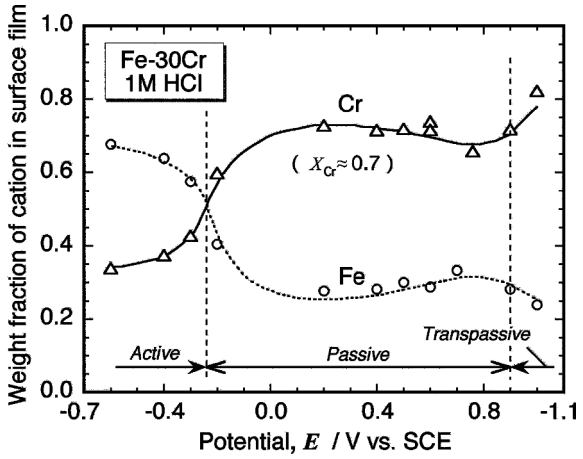

Fig. 1.2. Cationic mass fraction of elements as a function of potential for passive films formed on Fe-30Cr alloy in 1 M HCl [14]

film on the Fe-30Cr alloy reorganized from the original figure of Hashimoto et al. [14]. The cationic fraction of Cr, X_{Cr}, for passive films on Fe-30Cr alloy, which is immune against pitting, is approximately 0.7. On the other hand, that for passive films on the Fe-19Cr alloy, which is susceptible to pitting, is approximately 0.57 [16]. That is, the immunity against pitting in 1 M HCl can be attained at X_{Cr} = ca. 0.7. An explanation should be found for the question why the immunity against pitting is attained at X_{Cr} = ca. 0.7. The application of artificial passivation films, which are the analogue of passive films, is very convenient for examining the quantitative relationship between the composition and the function of films.

1.5 Fabrication of Artificial Passivation Films

Metallorganic chemical vapor deposition (MOCVD) [26, 27] and ion-beam sputter deposition (IBSD) [24, 25] have been employed for film formation. The former provides amorphous oxide films with higher OH^- content [5, 27]. However, it needs complicated control in order to obtain given composition and thickness. The latter gives amorphous oxide films with lower OH^- content but the control of composition and thickness is easy. Although the former is preferable from the viewpoint of the OH^- content, the latter has been commonly employed for ease in the control of composition and thickness.

In the formation of Fe_2O_3-Cr_2O_3 artificial passivation films by IBSD, high purity Ar is used for the ion source. A complex target is composed of a Cr_2O_3 plate and small Fe_2O_3 tablets. The maximum and the working degree of vacuum are 2.39×10^{-5} Pa and 1.46×10^{-2} Pa, respectively. The

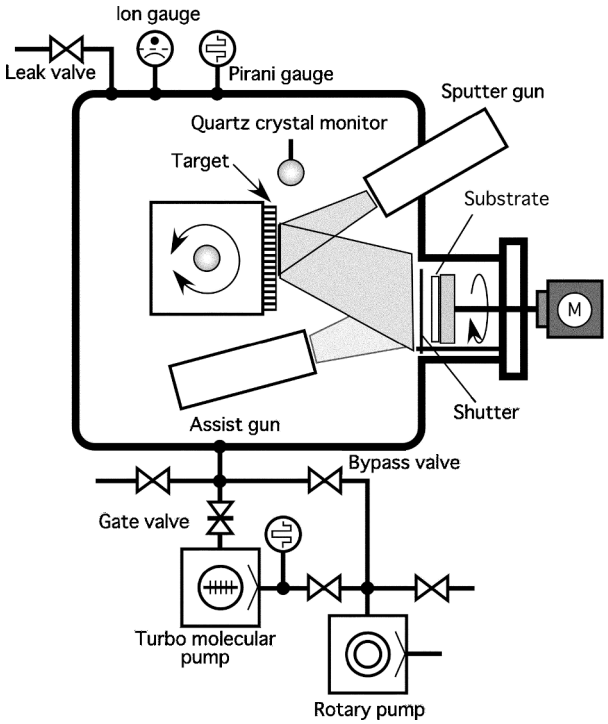

Fig. 1.3. Schematic diagram of ion-beam sputter deposition apparatus [28]

thickness of films formed is usually about 50 nm. The schematic diagram of the ion-beam sputtering system is given in Fig. 1.3 [28].

The chemical state of constituent elements in the film was analyzed by XPS. Figure 1.4 shows measured Fe 2p, Cr 2p and O 1s XPS spectra for Fe_2O_3-Cr_2O_3 films with X_{Cr} = 0.00–1.00 [28]. The films are composed of Fe^{3+} ions, Cr^{3+} ions, and O^{2-} ions with MO_x and $M(OH)_y$ type bonds (M: metal element). The deconvolution of Fe 2p and Cr 2p spectra revealed that Fe^{3+} ions exist as Fe_2O_3 and FeOOH type bonds and Cr^{3+} ions as Cr_2O_3 and $Cr(OH)_3$ type bonds [27, 28]. These chemical states of elements are just the same as those in real passive films [1].

AES depth profiles of elements in an Fe_2O_3-Cr_2O_3 film with X_{Cr} = 0.36 are shown in Fig. 1.5 [28]. The distribution of Fe, Cr and O content in the film is uniform from the top to the bottom of the film. Consequently, homogeneous films with given composition in the depth direction can be formed by IBSD.

From electron diffraction patterns and transmission electron micrographs, Fe_2O_3-Cr_2O_3 films with X_{Cr} larger than 0.35 are amorphous [28]. These films are not a mixture but a solid solution of Fe_2O_3 and Cr_2O_3.

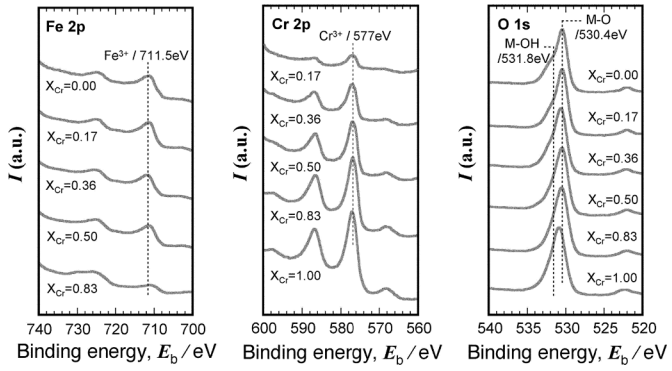

Fig. 1.4. XPS spectra for Fe_2O_3-Cr_2O_3 films with various X_{Cr} values [28]

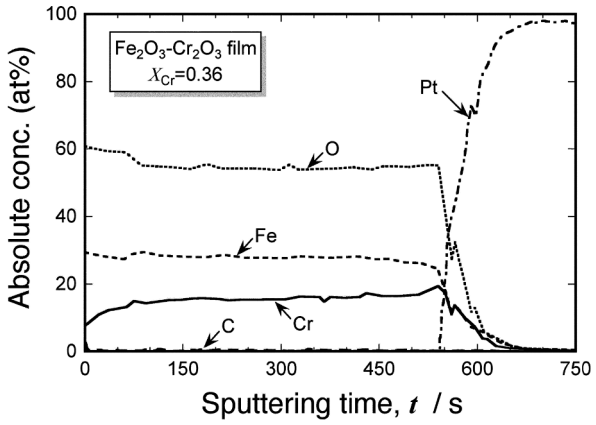

Fig. 1.5. AES in-depth profile of Fe_2O_3-Cr_2O_3 film with $X_{Cr} = 0.36$ [28]

1.6 Evaluation of Corrosion Resistance of Artificial Passivation Films

The electrochemical properties and corrosion resistance of Fe_2O_3-Cr_2O_3 films were examined by measuring the change in film thickness at various potentials in corrosive aqueous solutions using ellipsometry [4, 5]. This measurement technique is the same as that used for the measurement of thickness of passive films on stainless steels in solutions [1–3]. Figure 1.6 shows the schematic diagram of the apparatus used for the measurements [29]. The potential of specimens was controlled by a potentiostat in deaerated 1M HCl. The ellipsometric change in the surface of specimen was measured by a rotating analyzer type automatic ellipsometer. In the measurement and analysis, the three-parameter method was employed. That is, the relative phase retardation, Δ, the relative amplitude reduction, $\tan\Psi$, and the relative reflectivity, $\Delta R/R$, were measured and the thickness, d, and the optical constant,

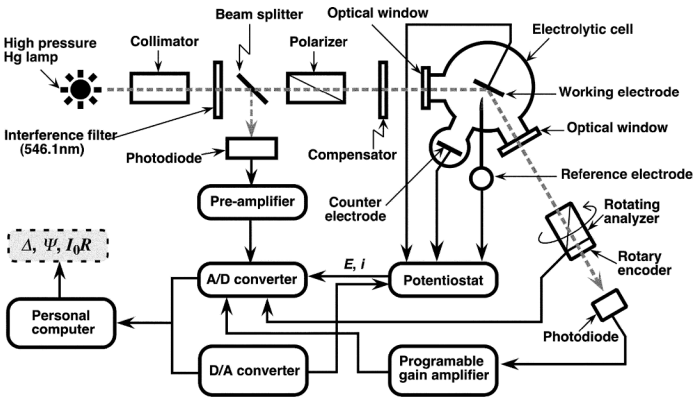

Fig. 1.6. Schematic diagram of electrochemical ellipsometric apparatus [29]

$N_2 = n_2 - k_2 i$, were calculated by Drude's optical equations using the three parameters measured. The thinning rate of film thickness was obtained from the gradient of decrease in film thickness vs time curve.

1.7 Dissolution Behavior of Fe_2O_3-Cr_2O_3 Films

Anodic and cathodic polarization curves of Fe_2O_3-Cr_2O_3 films with a series of X_{Cr} values in 1 M HCl at 298 K are shown in Fig. 1.7 [28]. The potential region under 0.5 V (vs Ag/AgCl, 3.33 M KCl) is the cathodic region. In this region, the films with X_{Cr} values of 0.00–0.50 show reductive currents at potentials from −0.2 V to 0.5 V. The increase in cathodic currents under −0.2 V is due to H_2 evolution. The potential region above 0.5 V is the anodic region. In the region of 0.5–1.0 V below the transpassive dissolution potential of Cr_2O_3-component, all films show very small currents corresponding to the passive current. That is, the Fe_2O_3-Cr_2O_3 films suffer from no pitting. Above 1.0 V, the films with X_{Cr} values of 0.17–1.00 show increases in anodic currents by the transpassive dissolution of the Cr_2O_3-component. The films with X_{Cr} values of 0.00–0.17 show Cl_2 evolution above 1.1 V and O_2 evolution above 1.5 V.

Figure 1.8 shows film thinning rate as a function of potential for the films in 1 M HCl [25]. Decreases in film thickness occur on the films with X_{Cr} values of 0.00–0.50 owing to the reductive dissolution of the Fe_2O_3-component ($Fe_2O_3 + 6H^+ + 2e^- \rightarrow 2Fe^{2+} + 3H_2O$) below 0.6 V. They also occur on the films with X_{Cr} values of 0.30–1.00 owing to the transpassive dissolution of the Cr_2O_3-component ($Cr_2O_3 + 4H_2O \rightarrow {Cr_2O_7}^{2-} + 8H^+ + 6e^-$) above 0.9 V. In the potential region between 0.6 V and 0.9 V there is no dissolution of any component of the films. Based on such a relationship between the thinning rate of film thickness and potential, the reductive dissolution region of the Fe_2O_3-component was designated as Region I, the region without dissolution

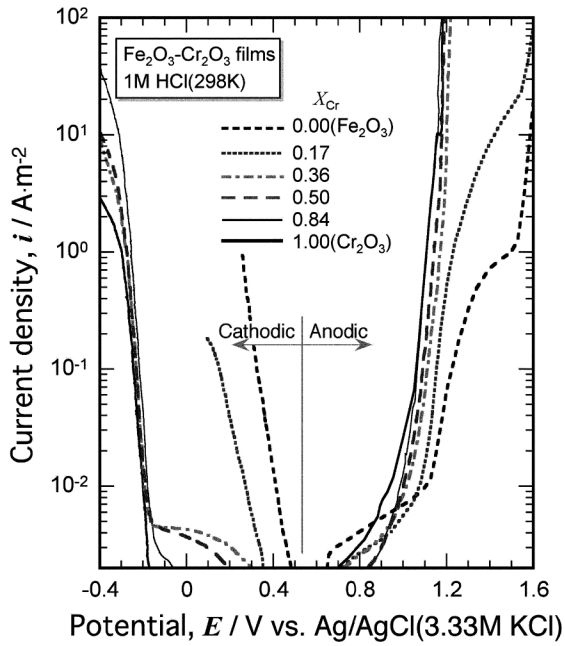

Fig. 1.7. Anodic and cathodic polarization curves of Fe_2O_3-Cr_2O_3 films in 1 M HCl [28]

as Region II, and the transpassive dissolution region of the Cr_2O_3-component as Region III. Region II is the intrinsic passivity region of Fe_2O_3-Cr_2O_3 films [30]. It is important that no pitting occurs on Fe_2O_3-Cr_2O_3 films in the anodic region.

In order to get the X_{Cr} value at which the reductive dissolution of the Fe_2O_3-component is suppressed, the relationship between the thinning rate of film thickness and the X_{Cr} value at -0.3 V in 1 M HCl is shown in Fig. 1.9. The thinning rate reached the analytical limit of ellipsometry at $X_{Cr} = 0.72$. That is, the Fe_2O_3-Cr_2O_3 films with X_{Cr} values larger than 0.72 cause no breakdown by reductive dissolution in 1 M HCl.

1.8 Anodic Polarization Behavior of Fe-Cr Alloys

Anodic polarization curves of high purity Fe-Cr alloys containing 10–30% Cr in 1 M HCl are shown in Fig. 1.10 [25]. This figure is similar to Fig. 1.1 but the purity of alloys used is much higher than those used for Fig. 1.1. As shown in Fig. 1.10, the alloys containing 10–25% Cr undergo pitting but the alloy containing 30% Cr does not suffer from pitting in this solution. This coincides well with the description of Fig. 1.1 [13–15]. The current density in the passive state of Fe-30Cr alloy is, however, unstable, showing that the

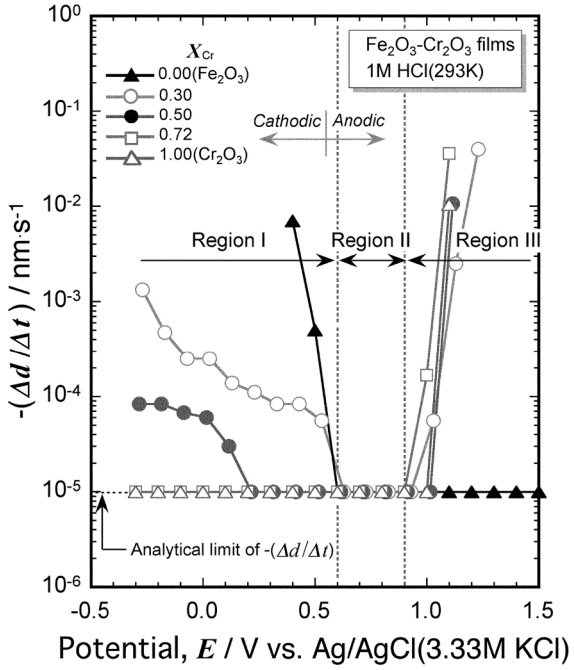

Fig. 1.8. Thinning rate of film thickness as a function of potential for Fe_2O_3-Cr_2O_3 films in 1M HCl [25]

passive film on the alloy has threshold composition for passivation in this solution. The three regions observed on the dissolution behavior of Fe_2O_3-Cr_2O_3 films were also present in Fig. 1.10. It should be noted that pitting occurs on low Cr alloys in Region I. That is, if part of a passive film has composition which is susceptible to reductive dissolution, that part should be broken down by reductive dissolution in the potential range of Region I.

1.9 Composition of Passive Films on Fe-Cr Alloys

In order to examine the change in the composition of passive films with potential, the surfaces of Fe-30Cr alloy treated at various potentials in 1M HCl for 3.6 ks were analyzed by Auger electron spectroscopy (AES) using Ar^+ ion sputtering at the same time. Figure 1.11 shows in-depth profiles of cationic mole fraction of elements in passive films [25]. It was found that the films formed at 0.3 V and 0.7 V have X_{Cr} values of about 0.6. This value is very close to the threshold value of 0.72, which is needed to suppress the reductive dissolution of the Fe_2O_3-component in Fe_2O_3-Cr_2O_3 films. The X_{Cr} values of the passive films on Fe-30Cr alloy are slightly lower than the threshold value. However, their real X_{Cr} values should be close to or higher than the threshold value because the AES signals of Fe and Cr from passive

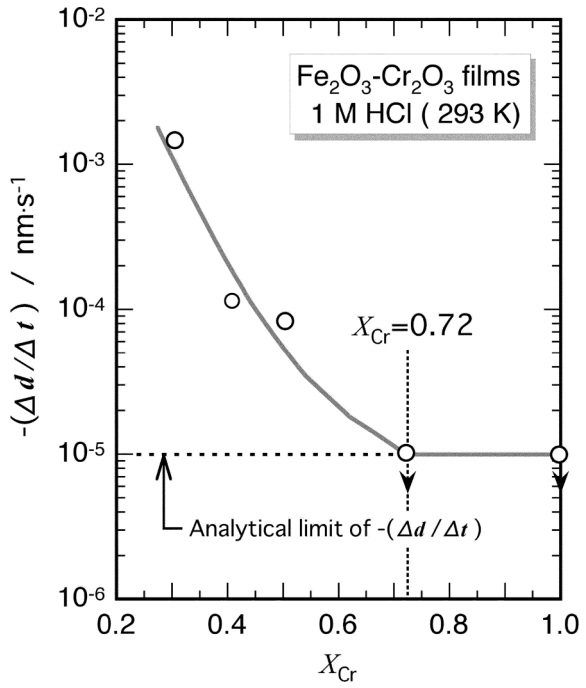

Fig. 1.9. Thinning rate of film thickness as a function of X_{Cr} value for Fe_2O_3-Cr_2O_3 films at −0.3 V in 1M HCl

films of about 2.7 nm thickness [14] under sputtering inevitably contain the signals from the alloy matrix and this sometimes makes the analytical values of Cr lower. Weight fractions of 0.6–0.7 have been reported for Cr cations in passive films on Fe-30Cr alloy at potentials between –0.16 V and 0.92 V in 1M HCl by quantitative XPS analysis without sputtering [14].

1.10 Comparison of Dissolution Behavior Between Fe_2O_3-Cr_2O_3 Artificial Passivation Film and Real Passive Film on Fe-Cr Alloy

Based on the dissolution behavior of Fe_2O_3-Cr_2O_3 film with potential, the passivation behavior of Fe-Cr alloy can be examined. Figure 1.12 compares the anodic polarization curve of Fe-30Cr alloy with the thinning rate vs potential curve of Fe_2O_3-Cr_2O_3 film with X_{Cr} = 0.72 in 1M HCl [25]. The composition of Fe_2O_3-Cr_2O_3 film simulates the threshold value which is needed to suppress the reductive dissolution of the Fe_2O_3-component in Fe_2O_3-Cr_2O_3 films in 1M HCl. It can be seen that the film with X_{Cr} = 0.72 hardly dissolves in the potential range between –0.3 V and 0.9 V, and this potential range corresponds well to the passivity region of Fe-30Cr alloy. From this fact, it

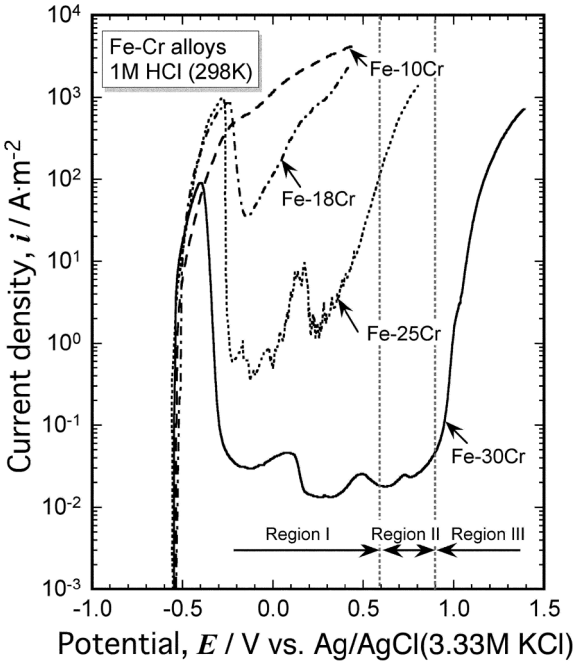

Fig. 1.10. Anodic polarization curves of high purity Fe-Cr alloys containing 10–30% Cr in 1 M HCl [25]

is thought that if the passive films contain an adequate amount of Cr_2O_3, which can suppress the dissolution in Region I, no pitting occurs on Fe-Cr alloys as Fe-30Cr alloy is stable up to 0.9 V in HCl.

1.11 Induction Period of Pitting on Fe-Cr Alloys

Since no dissolution occurs on Fe_2O_3-Cr_2O_3 films in Region II, there is a possibility that no pitting occurs on Fe-Cr alloys in this potential region. To substantiate this, induction periods for pitting were measured on Fe-20Cr alloy. In this measurement, the alloy was first passivated at given potentials in 1 M H_2SO_4 at 298 K for 18 ks and then the solution was switched over to 0.8 M H_2SO_4 + 0.4 M HCl + 0.6 M NaCl at 298 K while retaining the potentials. The induction time was defined as the time for the initiation of a continuous increase in current by pitting. Figure 1.13 shows the induction period for pitting as a function of potential [25]. Pitting started after a short time in the potential region between –0.1V and 0.3V. No initiation of pitting was observed up to 18 ks in the region between 0.5V and 0.7V. Pitting was observed at 0.9V due to the slight transpassive dissolution of passive film.

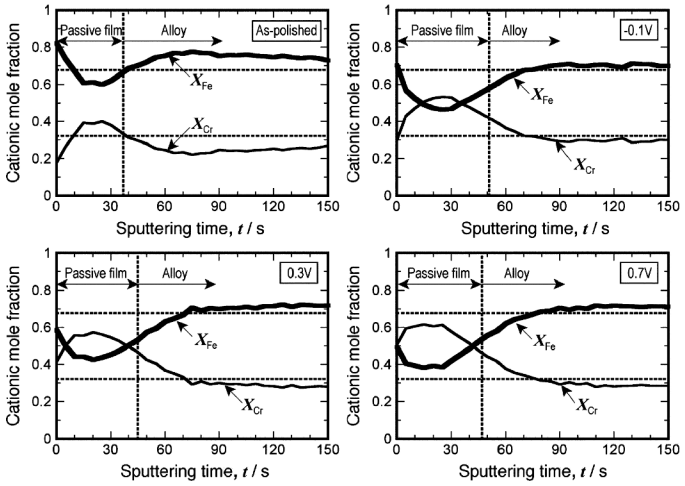

Fig. 1.11. AES in-depth profiles of cationic mole fraction of elements in passive films formed on Fe-30Cr alloy at various potentials in 1M HCl for 3.6 ks [25]

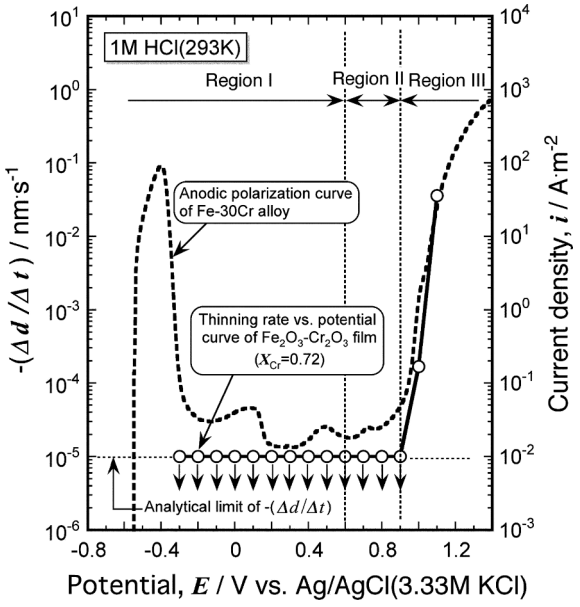

Fig. 1.12. Anodic polarization curve of Fe-30Cr alloy and thinning rate vs potential curve of Fe_2O_3-Cr_2O_3 film with $X_{Cr} = 0.72$ in 1M HCl [25]

That is, if a passive film is formed at a potential in Region II and then exposed to the Cl^--containing solution at the same potential, no pitting occurs [25].

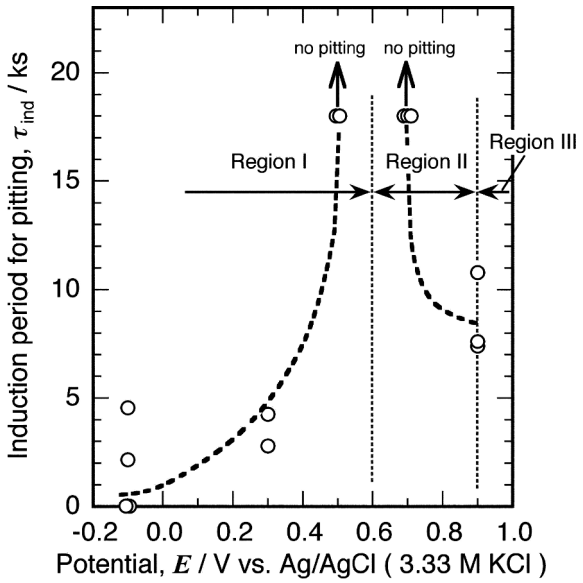

Fig. 1.13. Induction period for pitting as a function of potential for Fe-20Cr alloy first passivated in 1M H_2SO_4 and then kept in 0.8 M H_2SO_4 + 0.4 M HCl + 0.6 M NaCl [25]

1.12 Pitting Potentials of Fe-Cr Alloys in 1M HCl

In order to determine empirically the potential where pitting starts, pitting potentials of Fe-Cr alloys in 1M HCl reported in literatures [13, 14, 16, 24, 31, 32] were reviewed. Figure 1.14 shows pitting potential as a function of Cr content of alloys [25]. Almost all pitting potentials for Fe-Cr alloys containing 14–25% Cr exist between –0.23 V and 0.32 V, that is, in Region I. The pitting potentials for alloys containing 28–30% Cr jump up to over 0.98 V. Pitting potential is not the breakdown potential of passive film but the start potential of stable pitting. However, the breakdown potential should be very close to the pitting potential in a low pH and high Cl^- concentration environment such as 1 M HCl. The fact that pitting occurs in Region I suggests that, if the reductive dissolution of Fe_2O_3-component in passive films is suppressed, the breakdown of passive films, which leads to pitting, can be avoided [25].

1.13 Dissolution of Locally Heterogeneous Fe_2O_3-Cr_2O_3 Film

Since the reductive dissolution of low Cr_2O_3 concentration parts in passive films is thought to be responsible for pit initiation, an Fe_2O_3-Cr_2O_3 film with a low Cr_2O_3 concentration part was made and the dissolution behavior of the

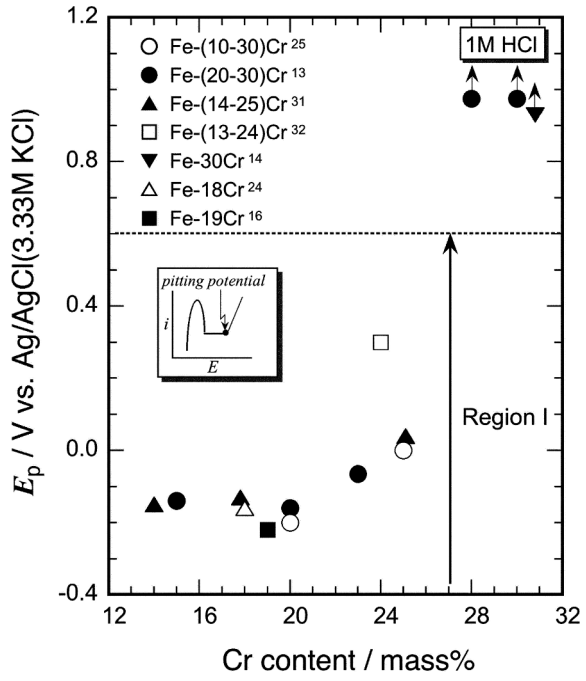

Fig. 1.14. Pitting potential as a function of Cr content for Fe-Cr alloys in 1M HCl reported in the literature [25]

film was examined at potentials in Regions I and II. Figure 1.15 shows optical micrographs of an Fe_2O_3-Cr_2O_3 film with a local part having $X_{Cr} = 0.24$ in a main part having $X_{Cr} = 0.76$ on a Type 304 substrate before and after potentiostatic polarization testing at –0.1V in Region I in 1 M HCl for 1.8 ks [25]. The diameter of the local part was 0.5 mm. The film of the local part was dissolved away after the polarization and the Type 304 substrate under the local part was severely pitted. An Fe_2O_3-Cr_2O_3 film with a local part having $X_{Cr} = 0.24$ in a main part having $X_{Cr} = 0.76$ was also made and tested at 0.7V in Region II in 1M HCl. The film of the local part was not dissolved at this potential [25].

1.14 Mechanism of pit Initiation on Fe-Cr Alloy

Based on the above discussion, the mechanism of pit initiation in an HCl solution can be presumed to be as shown in Fig. 1.16 [25].

In the case of low Cr alloys, the X_{Cr} value of passive films is not so high. Therefore, if the passive films have a localized Cr-depleted part, the X_{Cr} value of the part should be lower than the threshold X_{Cr} value that suppresses the reductive dissolution of Fe_2O_3-component in the films. Consequently, the Cr-depleted part causes the reductive dissolution at potentials in Region I. Since

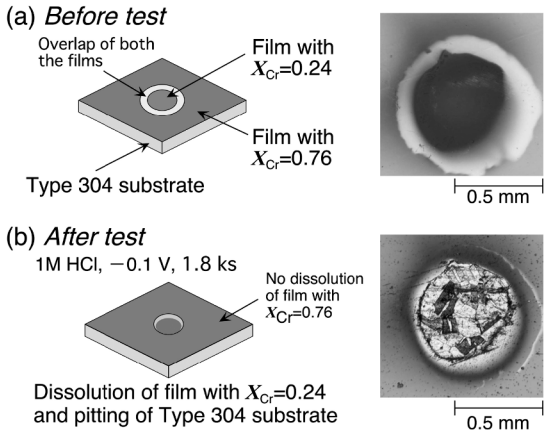

Fig. 1.15. Micrographs of Fe_2O_3-Cr_2O_3 film with locally low Cr_2O_3 concentration part on Type 304 substrate before and after polarization at −0.1 V in 1M HCl for 1.8ks [25]

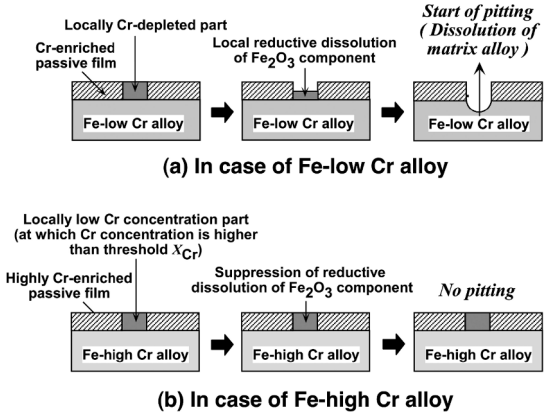

Fig. 1.16. Conceptional drawing of pit initiation mechanism on high purity Fe-Cr alloys in HCl solutions

the potentials in Region I for Fe-Cr alloys are anodic potentials (see Fig. 1.10), the alloy matrix exposed to an HCl solution by the local breakdown of passive film causes anodic dissolution. The anodic dissolution at the exposed part of the matrix continues because repassivation is impossible in this solution.

On the other hand, in case of high Cr alloys, the X_{Cr} value of passive films is high in general. Therefore, even if there is a localized Cr-depleted part in passive films, the X_{Cr} value of the part should be higher than the threshold X_{Cr} value. Consequently, the part causes no reductive dissolution at potentials in Region I and no pitting occurs at the part.

As stated before, pits are considered to initiate through the dissolution of sulfide inclusions in low purity Fe-Cr alloys [6–10]. Whether a pit repassivates or not in this case is dependent on the X_{Cr} value of passive film formed inside a pit. That is, if the X_{Cr} value exceeds the threshold value that is needed to suppress the reductive dissolution of the film in a solution with low pH and high Cl^- concentration inside a grown pit, the pit should be repassivated.

1.15 Summary

Film thinning rate as a function of potential for Fe_2O_3-Cr_2O_3 films in 1 M HCl shows the reductive dissolution region of the Fe_2O_3-component, no dissolution region of both the components, and the transpassive dissolution region of the Cr_2O_3-component. The reductive dissolution of the Fe_2O_3-component of the films can be suppressed by increasing Cr_2O_3 content.

Fe-30Cr alloy with a passive film having the threshold X_{Cr} value for suppression of the reductive dissolution of the Fe_2O_3-component suffers from no pitting in 1 M HCl. Fe-Cr alloys containing 14–25% Cr are susceptible to pitting in 1 M HCl and their pitting potentials exist in the reductive dissolution region of the Fe_2O_3-component in passive films. No initiation of pitting was observed on Fe-20Cr alloy in an acid solution containing 1 M Cl^- in the no dissolution region of both the components between 0.6V and 0.7V.

Potentiostatic polarization tests of Type 304 coated with a heterogeneous film with a localized small part of low Cr_2O_3 content in a wide matrix of high Cr_2O_3 content showed the initiation of pitting on the substrate Type 304 by the reductive dissolution of the small part in 1M HCl.

For the above reasons, the suppression of the reductive dissolution of the Fe_2O_3-component in passive films is presumed to be effective on the suppression of pitting in 1M HCl.

References

1. K. Sugimoto: Tetsu-to-Hagane, **70**, 637 (1984).
2. K. Sugimoto: Hyomen Kagaku, **9**, 61 (1988).
3. K. Sugimoto: Materia, **36**, 900 (1997).
4. K. Sugimoto: Materia, **34**, 1042 (1995).
5. K. Sugimoto: Zairyo-to-Kankyo, **47**, 616 (1998).
6. G. S. Eklund: J. Electrochem. Soc., **121**, 457 (1974).
7. S. E. Lott and R. C. Alkire: J. Electrochem. Soc., **136**, 973 (1989).
8. M. A. Baker and J. E. Castle: Corros. Sci., **34**, 667 (1993).
9. H. Böhni, T. Suter, and A. Schreyer: Electrochim. Acta, **40**, 1361 (1995).
10. D. E. Williams, T. F. Mohiuddin, and Y. Y. Zhu: J. Electrochem. Soc., **145**, 2664 (1998).
11. D. E. Williams, R. C. Newman, Q. Song, and R. G. Kelly: Nature, **350**, 216 (1991).

12. M. P. Ryan, N. J. Laycock, R. C. Newman, and H. S. Isaacs: J. Electrochem. Soc., **145**, 1566 (1998).
13. K. Sugimoto and Y. Sawada: Corros. Sci., **17**, 425 (1977).
14. K. Hashimoto, K. Asami, and K. Teramoto: Corros. Sci., **19**, 3 (1979).
15. K. Sugimoto, N. Hara, M. Isshiki, T. Ejima, and K. Igaki: J. Jpn. Inst. Metals, **46**, 703 (1982).
16. K. Hashimoto and K. Asami: Corros. Sci., **19**, 251 (1979).
17. A. R. Brooks, C. R. Clayton, K. Doss, and Y. C. Lu: J. Electrochem. Soc., **133**, 2459 (1986).
18. R. C. Newman, T. -M. Foong, and K. Sieradzki: Corros. Sci., **28**, 523 (1988).
19. S. Fujimoto, R. C. Newman, G. S. Smith, S. P. Kaye, H. Kheyrandish, and J. S. Colligon: Corros. Sci., **35**, 51 (1993).
20. A. J. Davenport, M. P. Ryan, M. C. Simmonds, P. Ermst, R. C. Newman, S. R. Sutton, and J. S. Colligon: J. Electrochem. Soc., **148**, B217 (2001).
21. U. Steinsmo and H. S. Isaacs: Corros. Sci., **35**, 83 (1993).
22. U. Steinsmo and H. S. Isaacs: J. Electrochem. Soc., **140**, 643 (1993).
23. W. P. Yang, D. Costa, and P. Marcus: J. Electrochem. Soc., **141**, 2669 (1994).
24. M. Son, N. Akao, N. Hara, and K. Sugimoto: J. Electrochem. Soc., **148**, B43 (2001).
25. K. Sugimoto, M. Son, Y. Ohya, N. Akao, and N. Hara: Corrosion Science – A Retrospective and Current Status in Honor of Robert P. Frankenthal, Electrochemical Society Proceedings Volume 2002-13, G. S. Frankel, H. S. Isaacs, J. R. Scully and J. D. Sinclair, Editors, p. 289, The Electrochemical Society, Pennington, (2002).
26. K. Sugimoto, M. Seto, S. Tanaka, and N. Hara: J. Electrochem. Soc. **140**, 1586 (1993).
27. H. Kim, N. Hara, and K. Sugimoto: J. Electrochem. Soc. **146**, 3679 (1999).
28. M. Son: Ph. D. Thesis, Tohoku University (2000).
29. K. Sugimoto: Electrochemistry, **62**, 212 (1994).
30. S. Tanaka, N. Hara, and K. Sugimoto: Mater. Sci. Eng. A, **198**, 63 (1995).
31. H. Chujo: Bachelor Thesis, Tohoku University (1998).
32. R. Goetz, J. Larrent, and D. Landolt: Corros. Sci., **25**, 1115 (1985).

http://www.springer.com/978-3-540-35177-1

Characterization of Corrosion Products on Steel Surfaces

Waseda, Y.; Suzuki, S. (Eds.)

2006, XVII, 297 p., Hardcover
ISBN: 978-3-540-35177-1